Int. J. Electrochem. Sci., 17 **(2022)** Article Number: 221187, doi: 10.20964/2022.11.82

International Journal of
ELECTROCHEMICAL
SCIENCE
www.electrochemsci.org

Novel Electrochemical Sensor Based on Acetylene Black for the Determination of Doxorubicin in Serum Samples

Shukai Sun[#,1], Xuanming Xu[#,1], Airong Niu[2], Zhixiang Sun[3], Yue Zhai[1], Shun Li[1], Chao Xuan[1], Yusun Zhou[1], Xiaomin Yang[1], Tingting Zhou[1,], Qingwu Tian[1,*]*

[1] Department of Clinical Laboratory, The Affiliated Hospital of Qingdao University, #No. 1677, Wutaishan Road, Qingdao 266000, Shandong, China
[2] Department of Laboratory Medicine, Qingdao Central Hospital, The Second Affiliated Hospital of Medical College of Qingdao University, Qingdao, Shandong Province, China
[3] Department of Clinical Laboratory, Qingdao Shinan District People's Hospital, Qingdao, Shandong Province, China
[#] These authors equally contributed to this work.
[*]E-mail: zhoutingting@qdu.edu.cn

Received: 8 September 2022 / *Accepted:* 9 October 2022 / *Published:* 20 October 2022

Doxorubicin (DOX) is an anthracycline antibiotic, which is clinically used for the chemotherapy of cancers. The monitoring of the concentration of DOX is important for the safety of treatment. In this study, a new glassy carbon electrode (GCE) comprising acetylene black (AB) as a sensitizer was developed for the determination of DOX in human serum. Cyclic voltammetry (CV) provided valuable information on electrode surface changes during fabrication. Electrochemical impedance spectroscopy (EIS) was applied to characterize the electrochemical properties of the prepared electrode. Parameters, such as scanning rate, AB volume, concentration, DOX enrichment time and pH, which affected the electrochemical determination of DOX, were optimized in detail. Under optimum conditions, the developed approach exhibited satisfactory selectivity, repeatability, and stability. In addition, the oxidative peak current was linearly proportional to the concentration of DOX in the ranges of 0.01–2.5 μM with a detection limit of 3.006 nM. Finally, the developed method was used for quantitative analysis of spiked humanserum samples, and the recovery was satisfactory (from 91.22% to 101.34%). Therefore, the prepared AB/GCE sensor could be applied for the analysis of DOX in real human serum samples.

Keywords: Acetylene black; Doxorubicin; Glassy carbon electrode; Electrochemical sensor

1. INTRODUCTION

DOX is also known as adriamycin, which belongs to the group of anthracycline antibiotics. In clinical settings, it is commonly used to treat breast cancer, ovarian cancer, soft tissue sarcomas, small cell lung cancer, multi-ple myeloma, and Hodgkin's lymphoma [1].

The mechanism of doxorubicin treatment is not clearly presented, but multiple explanations have been introduced for DOX-induced cellular apoptosis, such as the generating of free radicals, intercalation among DNA base pairs, inhibition the progression of enzyme topoisomerase II, induction of DNA double helix structure breaks and blocking the process of DNA replication [1, 2]. As an anticarcinogen, potential side-effects of DOX are evident, including cardiotoxicity effects, inhibition of bone marrow hematopoiesis, multiple-organ toxicity and gastrointestinal reactions [3-5]. Therefore, monitoring the concentration of DOX in serum could direct the use of drugs, minimize the toxicity of drugs, and ensure the drug safety of cancer patients and effectiveness of chemotherapy [6].

Based on available literature data, various methods for the determination of doxorubicin have been conducted such as high-performance liquid chromatography (HPLC) [7], fluorescence spectroscopy [8], and capillary electrophoresis [9]. Nevertheless, the large-scale application of the aforementioned strategies is strictly confined by a strenuous process, high cost and time consumption. By contrast, given their high sensitivity, satisfactory linear concentration range, miniaturization possibility, simple instrumentation, uncomplicated sample pretreatment procedures, and excellent performance of analysis [10], electrochemical techniques seem to be more simple, economical, and fast, which are suitable for biomarker analysis and clinical drug concentration detection [4, 11-14].

In general, conventional carbon electrodes, such as carbon paste, screen-printed carbon, graphite, and glassy carbon electrodes (GCE), have low electrical conductivity and poorredox and adsorption capacity. Modification on the surface of ordinary carbon electrodes is necessary to enhance the electrochemical activity of sensors to obtain better properties. Hence, several electrochemical materials are introduced into developed electrochemical sensors, including AB [13, 15-18]. AB with good electrical conductivity, high catalytic activity, large specific surface area, and strong adsorptive capacity for various samples is used in electrochemistry and electroanalysis [19, 20]. At present, AB has been extensively used for the determination of methotrexate [13], glucose [21], erythromycin [22], interleukin 6 [23], bisphenol A [20], and other substances. Meanwhile, inprevious work, a GCE has been developed to study the electrochemical behavior of DOX [24-26]. However, the preparation of electrochemical sensor AB combined with GCE for DOX determination has not been reported. Therefore, this work aimed to investigate the capabilities of AB/GCE for direct voltametric determination of an anticancer drug, such as DOX. Given its simple operation, less time, and low cost,AB/GCE-modified electrodes have a great application potential for detecting clinical drugs and formulating chemotherapeutic drugs forcancer therapies. Furthermore, the fabricated sensor was used to detect DOX in real serum samples.

2. MATERIALS AND METHODS

2.1. Chemicals

DOX was purchased from Exir Nano Sina Company (Tehran, Iran). Glycine, glucose, and citric acid were purchased from Solarbio (Beijing, China). Vitamin C, zinc sulfate, sodium chloride, potassium chloride, ferric chloride, and potassium ferrocyanide were supplied by Sinopharm Chemical Reagent Company (Shanghai, China). AB, N-doped carbon nanotube, single-walled carbon tube, multi-walled

carbon tube, grapheme, carboxyl carbon tube, molybdenum sulfide, amino carbon tube, single-layer carbon nano angle and hydroxyl carbon tube were purchased from STREM Chemicals, USA. DOX solution (1.0 μM) was prepared by dissolving DOX in methanol. Phosphate-buffered saline (PBS) of different pH values (0.1 M) was prepared with $Na_2HPO_4•12H_2O$ and $NaH_2PO_4•2H_2O$. The pH of PBS was adjusted by using hydrochloric acid and sodium hydroxide. Distilled water was used throughout the experiment.

2.2. Instruments

A CHI660C electrochemical workstation was used (Shanghai Chenghua Apparatus, Shanghai, China). A three-electrode system was composed of AB/GCE, saturated calomel electrode, and platinum electrode. A model 901 intelligent magnetic stirrer was purchased from San-Xin Instrumentation, (Shanghai, China) Inc. PHS-25 pH meter was obtained from INESA Scientific Instrument Company. (Shanghai, China).

2.3. Preparation of the modified electrode

First, 2.0 mg AB was added to 2.0 mL water and dispersed with ultrasonication for 1 h until a fine homogeneous black suspension was obtained. Then, the GCE was polished by using a polishing powder to remove any impurities. Subsequently, the electrode was ultrasonically purged in absolute ethyl alcohol and water for 2 min, until the electrode was as smooth as a mirror. Finally, 4.5 μL of the AB dispersion solution was dropped onto the surface of the GCE and dried to finish electrode modification.

2.4. Characterization of the AB electrochemical sensor

PBS (0.1 M, pH 7.0) was selected as an electrolyte solution for the detection of DOX.

50.0 μL of DOX (6.0 μM) was dissolved in the electrolyte solution, and smooth agitation was continued for 4 min. In addition, CV from 0.30 V to 1.0 V was recorded at a scanning rate of 100 mV s^{-1}. The detection of EIS was performed in 0.1 M KCl solution containing 5.0 mM $K_3Fe(CN)_6/K_4Fe(CN)_6$ with the frequency ranging in 0.01–100,000 Hz.

2.5. Standard solutions and serum sample preparation

The developed electrode was used to detect DOX in the human serum to verify its feasibility for application in real samples. The samples must be deproteinized before electrochemical detection to eliminate the interference of variouscomplex factors in serum. The method of pretreatment was based on the previous method by Deng with little modification[27]. Subsequently, 20.0 μL of purified samples was diluted to 10.0 mL of PBS, and DOX standard solutions of different concentrations (0.02, 0.5,1.0 and 2.0 μM) were added to the diluted samples for recovery experiments.

3. RESULTS AND DISCUSSION

3.1. Electrochemical behavior of DOX

Eminent materials with high absorptivity and electroconductibility are crucial for electrode preparation. The CV method was adopted into the experiment to study the electrochemical behavior of DOX on various electrodes. Fig. 1 shows the current response of DOX at different carbon-related electrodes. The current response of DOX on the AB-modified electrode was largest, which indicated that AB-modified electrode can signally enhanced adsorption and catalytic properties toward DOX compared with other material-modified electrodes. In addition, no reduction peak was observed in reverse scanning; thus, it confirmed the irreversibility of oxidation where DOX on the AB modified the electrode.

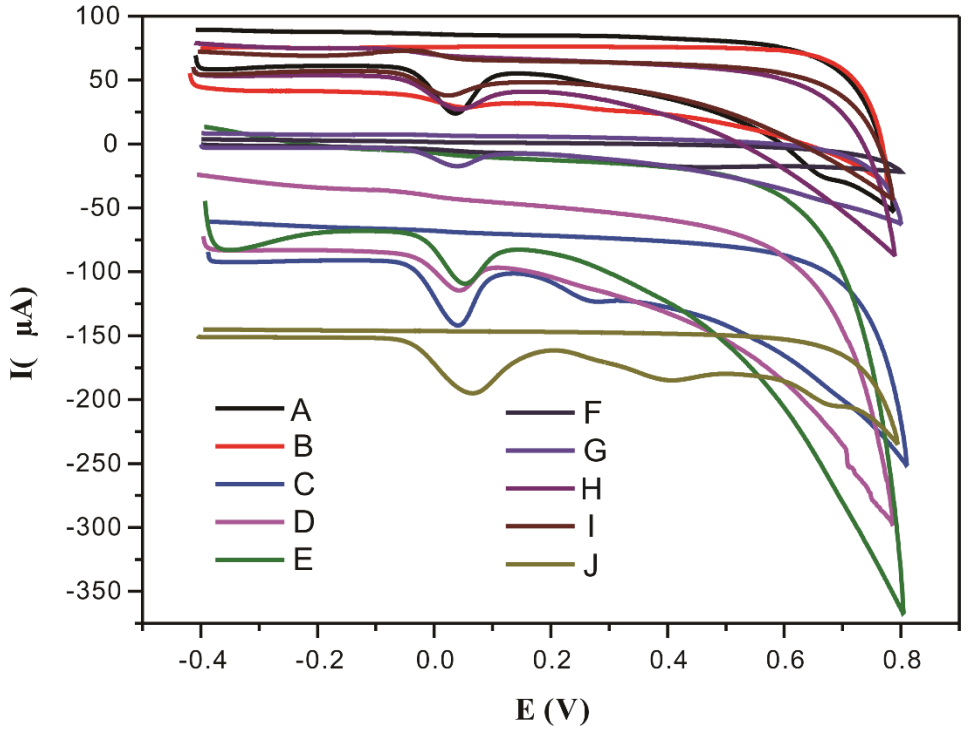

Figure 1. Cyclic voltammograms recorded at various catalytic materials on 1μM of DOX in 0.1M PBS buffer solution pH 7.0 (ν = 100mV s^{-1}). N-doped carbon nanotube (A), single-walled carbon tube (B), multi-walled carbon tube (C), grapheme (D), carboxyl carbon tube (E), molybdenum sulfide (F), amino carbon tube (G), single-layer carbon nano angle (H), hydroxyl carbon tube (I), AB (J)

3.2. Electrochemical characterization of the AB electrode

EIS is an efficient technique to investigate the electrochemical characteristics of electrodes. The Nyquist diagram of impedance spectra displays a semicircle part at higher frequencies, which is assigned to the limited transfer of electrons, and linear part at lower frequencies and associated with the diffusion [28, 29]. The diameter of semicircle illustrates thecharge transfer resistance (Rct), indicating the behavior of the electrode surface for the redox couple of the modification during every step; therefore, it can be

regarded as a signal to characterize the modification processes [30]. With $K_3[Fe(CN)_6]/K_4[Fe(CN)_6]$ as an indicator, resistance of the modified electrode was characterized using the EIS method in this work. The cyclic voltammogram (Fig. 2a) showed that the maximum oxidation peak current of curves AB/GCE and AB/GCE-DOX was larger than bare GCE and GCE-DOX. However, after adsorbing DOX on the electrode surface, the maximum oxidation peak current of curves GCE-DOX and AB/GCE-DOX were lower than before. The semicircle diameter of the Nyquist diagram presented the following pattern: GCE-DOX > GCE > AB/GCE-DOX > AB/GCE (Fig. 2b). Consequently, the modification of AB can considerably enhance the electrical conductivity of the electrode, thereby increasing the electron transfer speed of the prepared sensor. The result also indicated that adsorbed DOX on the electrode surface increased the transfer resistance of electron probably because of the passivation of surface with DOX binding, which was nonconducting.

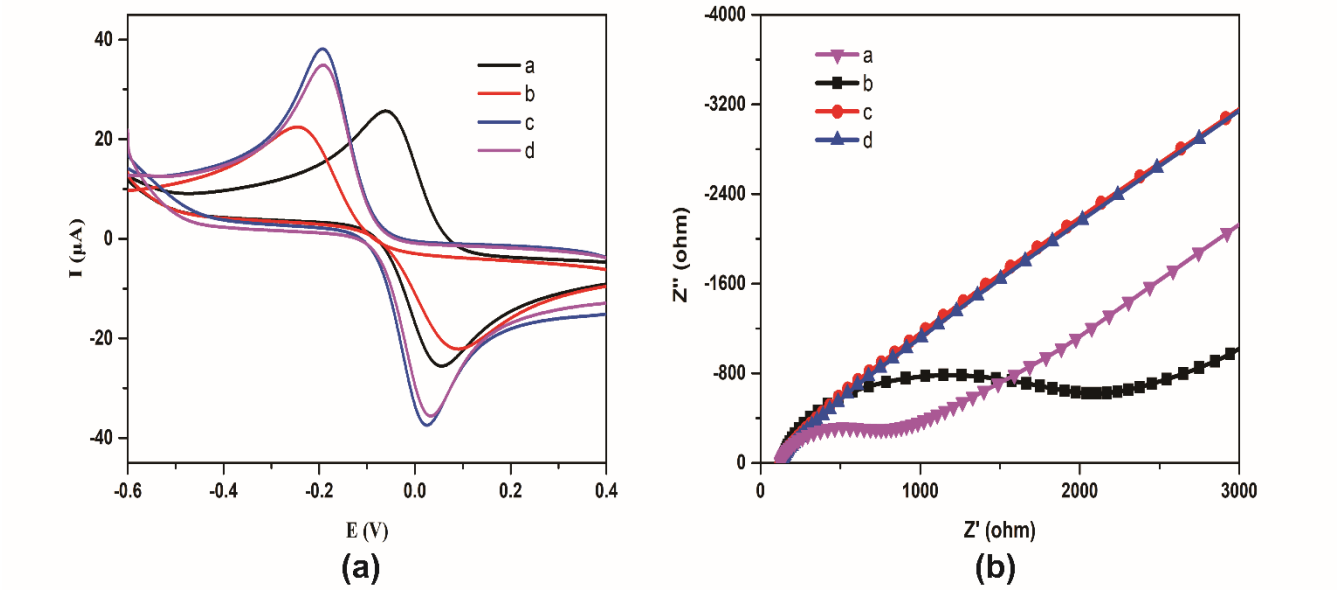

Figure 2. Cyclic voltammetry curves (a) and EIS curves (b) of GCE and AB/GCE before and after DOX adsorption in 5.0 mM $K_3Fe(CN)_6/K_4Fe(CN)_6$ solution. a: GCE, b: GCE-DOX, c: AB/GCE, d: AB/GCE-DOX.

3.3. Optimization of electrochemical experimental parameters

In the present study, the robustness of electroanalytical methods was dependent on several factors, which were relevant to the experimental parameters, such as AB dispersion volume, concentration, DOX enrichment time, pH, and scanning rate. Thus, the method should be robustly studied and should carefully select the experimental variables.

3.3.1. Effect of the AB dispersion volume on DOX detection

AB as the core material plays a vital role in this experiment. First, the responses of the volume ranging from 7.0–15.0 μL were recorded to investigate the effects of the volume of AB dispersion on the

oxidation peak current. Fig. 3a shows that as the volume increases in the range of 7.0 to 15.0 μL, the oxidation peak current of DOX reached the highest, where the volume was at 10.0 μL, and then achieved equilibrium state. However, in the actual experiments, the AB on the GCE could be shedded in certain degree during the volume above 10.0 μL. And the electrode surface could not be completely covered by AB when the volume of the AB solution was less than 10.0 μL, which resulted in the reduced adsorption and current response value of DOX on the electrode surface. Therefore, the best-shaped signal was obtained when the volume of AB was 10.0 μL, and this value was selected as optimal for subsequent studies.

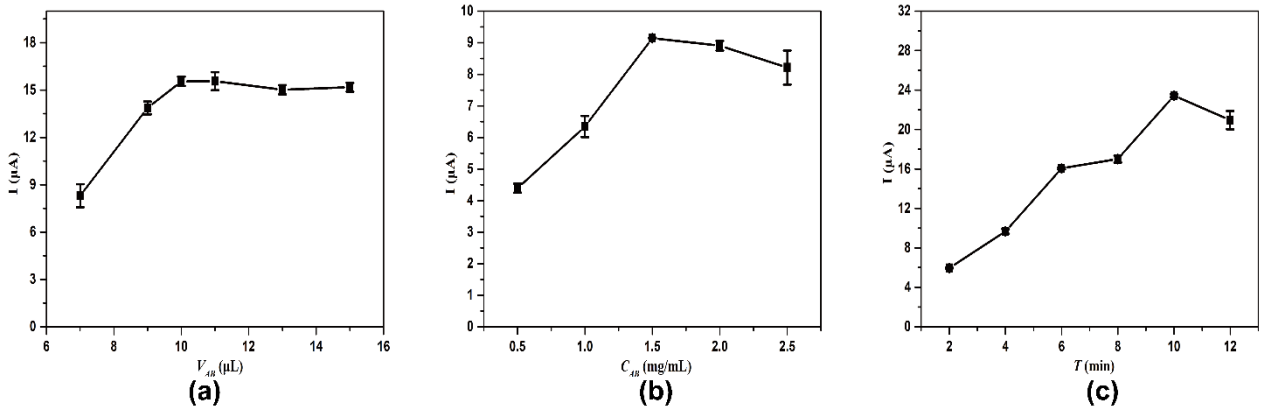

Figure 3. Effects of the AB volume (a), AB concentration (b) and DOX enrichment time (c) on the oxidation peak current of 1μM DOX in PBS (0.1 M, pH 7.0). Scanning rate: 100 mV s^{-1}.

3.3.2. Effect of AB concentration on DOX detection

Fig. 3b shows the correlation between different concentrations of AB and the oxidation peak current in 0.1 M PBS (pH of 7.0) solution containing 1.0 μM of DOX at scanning rate of 100 mV s^{-1}. As indicated in the figure, in the concentration range of 0.5–1.5 mg/mL, the oxidation peak current showed positive correlation and reached the maximum at 1.5 mg/mL,but the correlation had become negative thereafter because excessive AB on the electrode surface could affect the electron transmission between DOX and the catalyticelectrode, which resulted in a decrease in the oxidation peak current. Therefore, 1.5 mg/mLwas used as the optimal AB concentration in experiment.

3.3.3. Effect of DOX enrichment time on detection

Enrichment time can affect the catalysis of DOX on the electrode surface; thus, optimizing enrichment time is necessary to obtain a better experimental condition. As can be seen in Fig. 3c, the oxidation peak current increased with prolonged enrichment time and further increasing time decreased the DOX signal, which is due to electrode surface saturation[31]. Therefore, 10 min was selected as the optimal condition, indicating the adsorption efficiency of DOX was highest.

3.3.4. Effect of supporting electrolyte pH

The electrochemical oxidation of most organic compounds was affected by the solution pH, meanwhile, because the proton participated in the electrode reaction[32], so the influence of the supporting electrolyte pH on DOX oxidation peak was studied to identify the optimal experimental conditions for CV determination of DOX on AB/GCE. Based on the results (Fig. 4a), at pH 7.0, the maximum oxidation peak current was obtained. Meanwhile, a tendency toward a significant decrease in the peak height of DOX was observed when pH > 7.0.

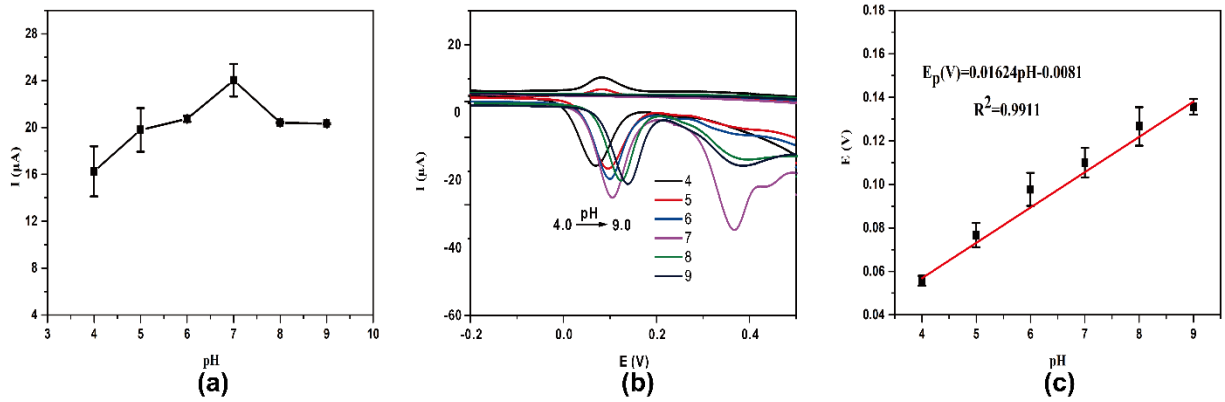

Figure 4. (a) Effects of buffer pH value on peak current. (b) Cyclic voltammograms of 1 μM DOX in PBS (0.1 M, pH7.0) on AB/GCE with pH ranging from 4.0 to 9.0. (c) Linear relationship between peak potential and buffer pH.

As shown in Fig. 4b, the influence of pH on the oxidative peak potential of 1 μM of DOX was investigated by performing CV analysis at different pH in the rang from 4.0 to 9.0. The peak potential could increase approximately and shift toward a more positive side with the increase of pH. Fig. 4c demonstrates the calibration curve for pH versus the peak oxidation potential. The linear regression equation for EP vs. the pH for DOX can be presented as EP (V) = 0.01624 pH−0.0081 with a correlation coefficient of R^2 = 0.9911 in the pH range of 4.0–9.0 and slope of 16.24 mV/pH. The theoretical value of Nernst's equation (−59 mV) was nearly 3.6 times that of the obtained slope (16.24 mV/pH), indicating that the number of electrons involved in DOX oxidation process was 3.6 times that of protons.

3.3.5. Influence of the scanning rate on the results

Although the effect of pH was evident, the influence of the scanning rate in the experiment cannot be ignored. The resultant linear regression equations obtained from the effect of scanning rate can be represented as I (μA) = 0.20731v+0.44572 (R^2=0.99547, Fig. 5a), in which the scanning rate was positively correlated with the oxidative peak current. In addition, E_P(V) = 0.02579lnv+0.04365 (R^2=0.99125, Fig. 5b) indicated that the peak potential was linearly related to the natural logarithm of the scanning rate. The abovementioned results indicated that the electrochemical behavior of the DOX

was in accordance with the diffusion-controlled process [33]. Considering that DOX on AB/GCE electrode showed a surface-controlled oxidation reaction, the oxidation peak potential and scanning rate of DOX on the AB/GCE electrode achieved the following Laviron formula [34]:

$E_P(V) = E^0+RT/(\alpha nF)\ln[RTk_s/(\alpha nF)]+RT/(\alpha nF)\ln\nu$,

where E^0 and k_S represent the standard potential and electron transfer rate constant, respectively. T represents the thermodynamic temperature (T=273.15+25 °C = 298.15 k). α represents the transfer coefficient set at 0.5 in the totally irreversible electrode process [35]. R represents molar gas constant (8.31 $J\cdot mol^{-1}\cdot k^{-1}$), F represents the Faraday constant (96485.33289 C/mol), and n represents the electron transfer number. Therefore, the number of electron transfer (n) transferred during DOX oxidation were nearly calculatedas 2.

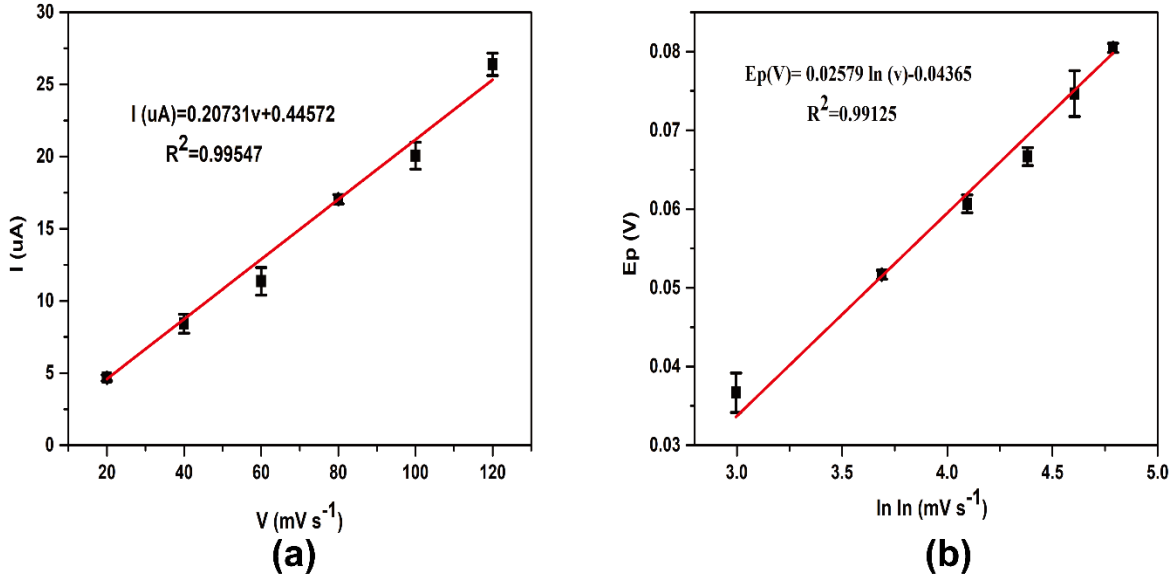

Figure 5. (a) Linear relationship between peak current and scanning rate. (b) Linear relationship between peak potential and the natural logarithm of the scanning rate (lnv).

3.4. Analytical performance of DOX

The CV curves of AB/GCE for different concentrations of DOX were recorded under optimized experimental conditions (Fig. 6a). The significant and rapid oxidative peak current enhancement was observed upon the gradual increase of the concentration of DOX. In addition, the linear equation between peak current intensity change and DOX concentration could be obtained as I(μA) = $18.542C_{DOX}$+0.22133 with a correlation coefficient of R^2 = 0.98747 (Fig. 6b) and linear range of 0.01−2.5 μM. The limit of detection (LOD) has been obtainedusing the general formula LOD=3*s*/*b*, where *s* indicates the relative standard deviation (RSD) of the cubic blank value, and *b* indicates the slope of the linear calibration curve [36, 37]. Therefore, the LOD is equal to 3.006 nM during this experiment.

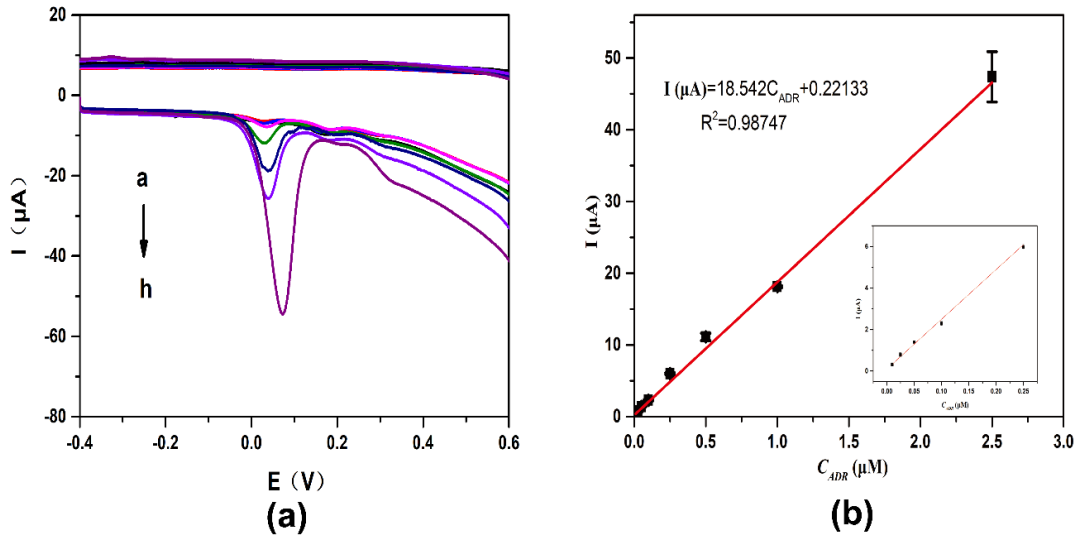

Figure 6. (a) CV curve of AB/GCE in diverse concentrations of DOX (from a to h): 0.01, 0.025, 0.05, 0.1, 0.25, 0.5, 1 and 2.5 μM. (b) Linear relationship between peak current and DOX concentrations.

A comparison of the analytical performance of previously reported methods and the proposed method for the determination of DOX is listed in Table 1. Comparedwith other DOX sensors, AB/GCE sensors had lower detection limit and a wider linear range of 0.01–2.5μM. Parameters such as repeatability (precision) and stability were estimated to verify the effectiveness of the prepared electrode. 1.0 μM of DOX was determined six times in 1 day on the same electrode, and the result showed an RSD of 3.25%. Producing the samemodified electrode per day, DOX was determined continuously for 1 week, and the RSD ofseven-time peak current was 4.68%. Therefore, the proposed electrode provided excellent repeatability and stability for the determination of DOX.

Table 1. Comparison of analysis from various reports with different selected materials and their respective LOD and linear range values toward the detection of DOX.

Sensors	Method	Linear Range(μM)	LOD (μM)	Reference
HMDE	SWV	0.5-10.0	0.1	[38]
PS/Fe_3O_4–GO–SO_3H–GCE	DPV	0.069–1.08	0.069	[39]
CD-GNs/GCE	DPV	10-0.2	100	[40]
OMWVCNT/GCE	SWV	0.04-90	0.009	[41]
TBSol–gel modified gold electrode	EIS and CV	4.0–8	1.5	[42]
AB/GCE	CV	0.01-2.5	0.003006	This work

DPV, differential pulse voltammetry; SWV, square wave voltammetry; HMDE, hanging mercury drop electrode; PS, polystyrene; GO, graphene oxide; SO3H, chlorosulfonic acid; OMWVCNT, oxidized multiwalled carbon nanotube; TBSol-gel, thiol base sol-gel.

3.5. Effect of interferents

In order to obtain the selectivity of the prepared sensor, the impact of potential interfering agents co-existing in human serum, including several inorganic ions and bioorganic molecules, was investigated, and the results were displayed in Table 2. Some exogenetic interference factors, which affected the electrochemical response, included 300-fold of Na^+, K^+, Cl^-, Zn^{2+}, SO_4^{2-}, vitamin C, and citric acid; 50-fold of Fe^{3+} and Fe^{2+}; and 20-fold of glycine and glucose. The interfering substances at these concentrations had no effect on the electrochemical responseof DOX. 1.0 μM of DOX with other interference analogs such as roxithromycin (ROX), clarithromycin (CRY), dirithromycin (DRY), and azithromycin (AZM) were tested to confirm the selectivity of the fabricated sensor. As shown in Fig. 7, the 20-fold or even 50-fold higher concentration of the four different drugs hardly affected the current response of DOX. This result indicated that the proposed sensor could be used to analyze DOX in real samples, even in the presence of a high concentration of interferents, thereby indicating the superior selectivity and anti-interference of the sensor toward the voltametric determination of DOX.

Table 2. Interference levels of several substances in the determination of 1.0 μM of DOX.

Substances	Interference Level
Na^+, K^+, Cl^- , Zn^{2+}, SO_4^{2-}, vitamin C, citric acid	300
Fe^{3+}, Fe^{2+},	50
Glycine, Glucose,	20

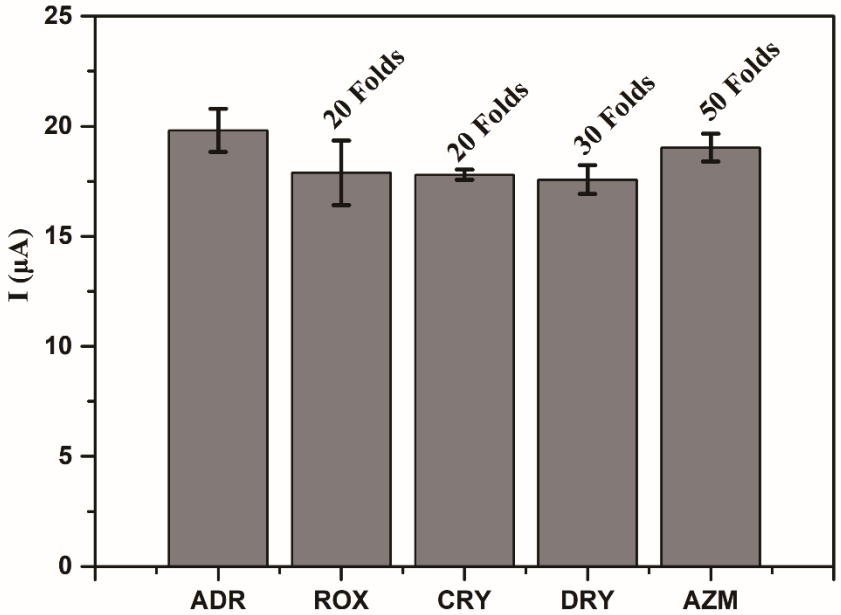

Figure 7. The current plots at AB/GCE in the presence of 1.0 μM DOX with different interference analogues.

3.6. Detection of DOX in human serum samples

Under optimum experimental conditions, human serumsamples were analyzed to consider the feasibility of electrode determination. Table 3 shows more than 91.22% recovery of the analyzed samples, and the four-time measurement value of DOX was lower than 2.0%. The obtained results demonstrated that the proposed methodology using AB/GCE was applicable for the detection of DOX in biological samples in clinical settings.

Table 3. Determination of DOX in human serum at AB/GCE

Added (μM)	Found (μM)	Recovery (%)	RSD (%) (n=6)
0.02	0.0188	94.10%	0.0264
0.5	0.4560	91.22%	0.2072
1.00	1.0434	104.34%	0.2333
2.00	1.9624	98.12%	1.1313

4. CONCLUDING REMARKS

This work provided comprehensive understanding of AB as an innovative sensor for the determination of antitumor drugs. Simple ultrasonication was used for the preparation of AB/GCE, which exhibited an effective electro-catalytic performance with enhanced selectivity, stability, and repeatability. At the optimal experimental conditions, the new electrochemical method exhibited lower LOD (3.006 nM) and wider linear range (0.01–2.5 μM) demonstrating the high sensitivity of the electrode. The newly fabricated sensor can be utilized for detecting lower concentrations of DOX without other tedious pre-treatment. Moreover, AB/GCE can be an efficient electrochemical instrument for the detection of DOX in human serum with high recovery of 91.22%–104.34% and RSD ranging from 0.0264% to 1.1313%. In this case, AB-based tools should be further regarded as advantageous for the sensitive monitoring of clinical chemotherapeutic medicines.

Conflicts of interest

There are no conflicts to declare.

Data Availability Statement

Data will be made available on reasonable request.

Acknowledgments

This research was funded by the National Natural Science Foundation of China (No. 81802107) and the Natural Science Foundation of Shandong Province (No. ZR2019BH053). We thank all participants for their involvement in our study.

References

1. S. Rivankar, *J. Cancer Res. Ther.*, 10 (2014) 853-8.

2. M. Baxter-Holland and C. R. Dass, *J. Pharm. Pharmacol.*, 70 (2018) 320-327.
3. F. Chekin, V. Myshin, R. Ye, S. Melinte, S. K. Singh, S. Kurungot, R. Boukherroub and S. Szunerits, *Anal. Bioanal. Chem.*, 411 (2019) 1509-1516.
4. J. Liu, X. Bo, M. Zhou and L. Guo, *Mikrochim. Acta*, 186 (2019) 639.
5. I. Rus, M. Tertiș, C. Barbălată, A. Porfire, I. Tomuță, R. Săndulescu and C. Cristea, *Biosensors (Basel).*, 11 (2021).
6. F. Meng, F. Gan and G. Ye, *Mikrochim. Acta*, 186 (2019) 371.
7. S. I. Aboras, M. A. Korany, H. H. Abdine, M. A. A. Ragab, A. El Diwany and M. M. Agwa, *J. Chromatogr. B: Anal. Technol. Biomed. Life Sci.*, 1187 (2021) 123043.
8. J. S. Pérez-Blanco, M. Fernández de Gatta Mdel, J. M. Hernández-Rivas, M. J. García Sánchez, M. L. Sayalero Marinero and F. González López, *J. Chromatogr. B: Anal. Technol. Biomed. Life Sci.*, 955-956 (2014) 93-7.
9. S. M. Ansar and T. Mudalige, *Int. J. Pharm.*, 561 (2019) 283-288.
10. M. Ramya, P. Senthil Kumar, G. Rangasamy, V. Uma shankar, G. Rajesh, K. Nirmala, A. Saravanan and A. Krishnapandi, *Chemosphere*, 308 (2022) 136416.
11. P. Bollella, G. Fusco, C. Tortolini, G. Sanzò, G. Favero, L. Gorton and R. Antiochia, *Biosens. Bioelectron.*, 89 (2017) 152-166.
12. A. Ravalli, D. Voccia, I. Palchetti and G. Marrazza, *Biosensors (Basel).*, 6 (2016).
13. Z. Deng, *Int. J. Electrochem. Sci.*, (2020) 5058-5066.
14. H. Ibrahim and Y. Temerk, *Mikrochim. Acta*, 187 (2020) 579.
15. B. Huang, L. Xiao, H. Dong, X. Zhang, W. Gan, S. Mahboob, K. A. Al-Ghanim, Q. Yuan and Y. Li, *Talanta*, 164 (2017) 601-607.
16. R. Cazelles, R. P. Shukla, R. E. Ware, A. A. Vinks and H. Ben-Yoav, *Biomedicines*, 9 (2020).
17. Z. Rezaeifar, G. H. Rounaghi, Z. Es'haghi and M. Chamsaz, *Mater. Sci. Eng., C*, 91 (2018) 10-18.
18. Y. Cao, L. Wang, C. Shen, C. Wang, X. Hu and G. Wang, *Sens. Actuators, B*, 283 (2019) 487-494.
19. P. Deng, Z. Xu and Y. Feng, *Mater. Sci. Eng., C*, 35 (2014) 54-60.
20. W. Xu, F. Yuan, C. Li, W. Huang, X. Wu, Z. Yin and W. Yang, *J. Sep. Sci.*, 39 (2016) 4851-4857.
21. X. Gao, W. Feng, Y. Xu, Y. Jiang, C. Huang, Y. Yi, A. Guo, X. Qiu and W. Chen, *Nanoscale Res. Lett.*, 15 (2020) 23.
22. X. Hu, P. Wang, J. Yang, B. Zhang, J. Li, J. Luo and K. Wu, *Colloids Surf., B*, 81 (2010) 27-31.
23. E. B. Aydın, M. Aydın and M. K. Sezgintürk, *Talanta*, 222 (2021) 121596.
24. M. Hasanzadeh, N. Hashemzadeh, N. Shadjou, J. Eivazi-Ziaei, M. Khoubnasabjafari and A. Jouyban, *J. Mol. Liq.*, 221 (2016) 354-357.
25. Y. Guo, Y. Chen, Q. Zhao, S. Shuang and C. Dong, *Electroanalysis*, 23 (2011) 2400-2407.
26. J. Fei, X. Wen, Y. Zhang, L. Yi, X. Chen and H. Cao, *Microchim. Acta.*, 164 (2008) 85-91.
27. Z. Deng, H. Li, Q. Tian, Y. Zhou, X. Yang, Y. Yu, B. Jiang, Y. Xu and T. Zhou, *Microchem. J.*, 157 (2020) 105058.
28. S. K. D. Vishnu, P. Ranganathan, S. P. Rwei, C. Pattamaprom, T. Kavitha and P. Sarojini, *Int. J. Biol. Macromol.*, 148 (2020) 79-88.
29. T. Zhou, X. Zhao, Y. Xu, Y. Tao, D. Luo, L. Hu, T. Jing, Y. Zhou, P. Wang and S. Mei, *RSC Adv.*, 10 (2020) 2123-2132.
30. B. Rezaei, N. Askarpour and A. A. Ensafi, *Talanta*, 119 (2014) 164-9.
31. B. Hassan Pour, N. Haghnazari, F. Keshavarzi, E. Ahmadi and B. Rahimian Zarif, *Microchem. J.,* 165 (2021) 106147.
32. P. Shi, X. Miao, H. Yao, S. Lin, B. Wei, J. Chen, X. Lin and Y. Tang, *Electrochim. Acta*, 92 (2013) 341-348.
33. A. V. Ivanishchev, A. V. Churikov, I. A. Ivanishcheva and A. V. Ushakov, *Ionics*, 22 (2015) 483-501.
34. J. M. Chrétien, M. A. Ghanem, P. N. Bartlett and J. D. Kilburn, *Chemistry*, 14 (2008) 2548-56.
35. J. Waelder and S. Maldonado, *Anal. Chem.*, 93 (2021) 12672-12681.

36. H. Y. Aboul-Enein, *Chromatographia*, 75 (2012) 811-811.
37. B. Uno, *Anal. Bioanal. Chem.*, 408 (2016) 4825-4826.
38. Y. Hahn and H. Y. Lee, *Arch. Pharmacal Res.*, 27 (2004) 31-4.
39. J. Soleymani, M. Hasanzadeh, N. Shadjou, M. Khoubnasab Jafari, J. V. Gharamaleki, M. Yadollahi and A. Jouyban, *Mater. Sci. Eng., C*, 61 (2016) 638-50.
40. J.-G. Guan, Y.-Q. Miao and Q.-J. Zhang, *J. Biosci. Bioeng.*, 97 (2004) 219-226.
41. E. Haghshenas, T. Madrakian and A. Afkhami, *Anal. Bioanal. Chem.*, 408 (2016) 2577-86.
42. K. Hirano, T. Nagae, T. Adachi, Y. Ito and M. Sugiura, *J. Pharmacobio-Dyn,* 6 (1983) 588-94